

1 Symbiont community changes confer fitness benefits for larvae, but not juveniles, in a vertically
2 transmitting coral

3 Daniel Olivares-Zambrano^{1,*}, Courtney Timmons¹, Carly D. Kenkel¹, Kate M. Quigley^{2,3}

4 ¹Department of Biological Sciences, University of Southern California, Los Angeles CA, USA

5 ²Minderoo Foundation, Perth, WA 6009, Australia

6 ³James Cook University, Townsville, QLD, 4810, Australia

7

8

9

10

11

12

13

14

15

16

17

18

19

20

21

22

23

24

25

26 *Correspondence: Email: Dannyolizam@gmail.com

27 Running head: Transgenerational shuffling across multiple life-stages

28

29 Keywords: transgenerational acclimatization, heat stress, Symbiodiniaceae, coral reefs,
30 symbiosis

31

32

33

34

35

36

37

38

39

40

41

42

43

44

45

46

47

48

49

50

51

52

53 **Abstract**

54 Coral reefs worldwide are threatened by increasing ocean temperatures because of the sensitivity
55 of the coral-algal symbiosis to thermal stress. Reef building corals form mutualistic symbiotic
56 relationships with dinoflagellates (family Symbiodiniaceae), including those species which
57 acquire their initial symbiont complement from their parents. Changes in the composition of
58 symbiont communities, through the mechanisms of symbiont shuffling or switching, can modulate
59 thermal limits. However, the role of shuffling in coral acclimatization is understudied and work to
60 date has largely focused on adults. To quantify the fitness consequences of changes in symbiont
61 communities under a simulated heatwave in early life-history stages, we exposed the larvae and
62 juveniles of the widespread, vertically transmitting coral *Montipora digitata* to heat stress (32°C)
63 and tracked changes in their growth, survival, photosynthetic efficiency, and symbiont community
64 composition relative to controls. We found negative impacts with warming in all fitness-related
65 traits, which varied significantly among larval families and life-stages. Surviving larvae exposed
66 to heat exhibited changes in symbiont communities that favoured types that are canonically more
67 stress tolerant. Compared to larvae, juveniles showed more rapid mortality under heat stress and
68 their symbiont communities were largely fixed regardless of temperature treatment, suggesting an
69 inability to alter their symbiont community as an acclimatory response to heat stress. Taken
70 together, these findings suggest that capacity for symbiont shuffling may be modified through
71 development, and that the juvenile life-stage is more at risk from climate warming.

72

73

74

75

76

77

78

79

80

81

82

83

84

85 Introduction

86 Symbiosis is a fundamental biological process in the oceans. Across the tree of life,
87 symbiosis fuels biodiversity and many species engage in these life-long partnerships to increase
88 their fitness through mechanisms like nutrient exchange, shelter, or chemical defenses (Sachs et
89 al. 2004). However, symbiotic relationships are not always equitable or stable over ecological
90 timescales and benefit sharing between host and symbiont can change with varying environmental
91 conditions - like warming (Kiers et al. 2003; Kiers et al. 2010). The nutritional exchange
92 underpinning life on coral reefs, the coral-algal symbiosis, is particularly sensitive to
93 environmental perturbation (Davy. et al. 2012).

94 Coral bleaching is defined as the breakdown of the partnership between photosynthetic
95 dinoflagellate symbionts (Symbiodiniaceae) and their coral hosts from environmental stress.
96 Generally, this can be caused by high and persistent temperature and high light (van Woesik 2001).
97 If stressful conditions persist, this can result in mortality of the host due to the loss of symbiont-
98 derived nutrition or destruction of host tissues (Glynn 1993). Ocean warming currently represents
99 the greatest threat to the persistence of coral reefs globally (van Woesik et al. 2022). As the main
100 driver of warming, human induced climate change is increasingly leading to more severe and
101 frequent bleaching and mortality events on reefs (van Woesik et al. 2022). However, there is
102 variation in bleaching susceptibility among individuals, populations, and species attributable to a
103 variety of genetic and non-genetic mechanisms (Voolstra et al. 2021). One key driver of this
104 variation in heat tolerance is the composition of Symbiodiniaceae in the coral (Baker 2004;
105 Berkelmans and van Oppen 2006; Fuller et al. 2020).

106 Dinoflagellates in the family Symbiodiniaceae are classified into 10 genera with most,
107 except for the lone species in the genus *Effrenium*, capable of forming a symbiosis with coral
108 (LaJeunesse et al. 2018; Yorifuji et al. 2021). Corals vary in the degree of specificity in their
109 symbiotic partnerships (Sampayo et al. 2016; Elder et al. 2023) and the range of potential
110 Symbiodinaceae partners is diverse (LaJeunesse et al. 2018). Some hosts maintain simultaneous
111 relationships with multiple symbionts, whereas others are more specific (Davies et al.
112 2023). Importantly, differences in these communities drive variation in host fitness, including heat
113 and light tolerance, and growth rates (Putnam et al. 2012; Swain et al. 2017; Cunning et al. 2018;
114 Matsuda et al. 2022; Davies et al. 2023). For example, an increase in the relative abundance of
115 *Durusdinum trenchii* (formerly D1a, LaJeunesse et al. 2018) in three coral species resulted in
116 increased heat tolerance (Cunning et al. 2018).

117 In addition to their phylogenetic diversity, the coral-Symbiodinaceae symbiosis can be
118 modified through the ecological mechanisms by which corals acquire and dynamically regulate
119 their symbiont communities which also influences thermal resistance and resilience of the
120 holobiont. There are two main mechanisms by which symbiont communities change *in hospite*,
121 namely shuffling and switching. Symbiont shuffling refers to changes in the relative abundance of
122 community members already in residence (Baker 2001; Baker et al. 2004). Generally, this involves
123 a reduction in the abundance of a dominant symbiont due to an environmental change which
124 provides an opportunity for a numerically rarer symbiont(s) to increase in relative abundance
125 (Quigley et al. 2022). This process should, by definition, result in an increase in host fitness and
126 may be adaptive (Baker et al. 2004). Switching refers to the ability of a host to replace an existing

127 symbiosis by selecting for a novel partner from the environment (Sørensen et al. 2021). Increased
128 abundance of symbionts in the opportunistic and generally stress tolerant genus *Durusdinium* is
129 the canonical example of shuffling following heat stress (Berkelmans and van Oppen 2006;
130 Quigley et al. 2022), again emphasizing the role of symbionts in reef resilience (Berkelmans and
131 van Oppen 2006; Quigley et al. 2022). However, our knowledge of the functional relevance of
132 shuffling and switching is generally limited to adult coral and has only been briefly examined in
133 early life-history stages (Quigley et al. 2019; Terrell et al. 2023).

134 Symbiont communities in adult corals are also influenced by the mode of symbiont
135 acquisition (Fabina et al. 2012). In corals, there are three known mechanisms for symbiosis
136 initiation: vertical, horizontal, or mixed-mode, with the majority of coral employing horizontal
137 transmission (Quigley et al. 2018; Baird et al. 2009). Horizontally transmitting corals must acquire
138 their algal symbionts from the environment each generation. Vertical transmitters, on the other
139 hand, obtain their symbiont community from a maternal source, often through the infection of
140 oocytes before fertilization or planula during gestation (Davy and Turner 2003; Hirose and Hidaka
141 2006; Padilla-Gamiño et al. 2012). Mixed mode transmission refers to the ability for corals to
142 inherit their symbiont community from a maternal source with the additional ability to acquire
143 symbionts from the environment during development (Ebert 2013). Thus far, coral species have
144 generally been categorically described as either vertical or horizontal transmitters (Baird et al.
145 2009), although mixed mode transmission was recently described in a canonical vertical
146 transmitter (Quigley et al. 2018).

147 A better understanding of transmission mode is critical because it affects the long-term
148 fidelity of the symbiotic association (Ebert 2013; Quigley et al. 2018; Dixon and Kenkel 2019).
149 Vertically transmitted symbioses are generally thought to be co-evolved associations, in which the
150 diversity of symbionts in the host coral is lower (Fabina et al. 2012), and the ability of the symbiont
151 to live outside the host is restricted (Krueger and Gates 2012). However, in the vertically
152 transmitting coral *Montipora digitata*, symbiont communities in offspring are more diverse
153 compared to adults (Quigley et al. 2017), and alterations in symbiont community composition in
154 adults due to stress are reflected in oocytes, supporting the potential for transgenerational
155 inheritance of shuffled algal communities over time (Quigley et al. 2019). This suggests that
156 vertically transmitted symbiont communities are more flexible than originally thought and
157 dynamic shifts in the complement of algal symbionts passed on to offspring may confer fitness
158 benefits in variable environments (Björk et al. 2019).

159 Taken together, there is now evidence that flexible symbiotic partnerships may confer
160 greater adaptive and acclimatory potential on the coral holobiont (Torda et al. 2017). However, the
161 majority of our current understanding regarding the fitness impacts of flexible symbiont
162 associations comes from studies on adult life stages (Baker 2001; Berkelmans and van Oppen
163 2006; Mieog et al. 2007). Larval life stages of marine invertebrates have higher energetic demands
164 (Pechenik 1999), making nutritional endosymbionts even more essential, particularly for vertically
165 transmitting coral species. In addition, the physiological consequences of the transgenerationally
166 inherited community shifts observed in oocytes on later coral life-stages remains unknown
167 (Quigley et al. 2019). To evaluate the relationship between physiological metrics of fitness and
168 symbiont community composition over coral ontogeny, we exposed multiple cohorts of coral
169 larvae and juveniles to heat stress and monitored changes in their physiology, survival and
170 Symbiodiniaceae communities over time. In addition to reductions in photosynthetic efficiency of

171 symbionts, and size and survival of the host, we show that heat stress in larval samples increased
172 Symbiodiniaceae community alpha diversity through increasing abundances of *Symbiodinium*,
173 *Durusdinium* and *Fugacium* spp. Heat stressed juveniles on the other hand, showed a limited
174 capacity to shuffle their symbiont communities. Finally, we show that increased community
175 diversity of Symbiodiniaceae in maternal coral is reflected in a family of offspring and may have
176 fitness consequences.

177 **Materials and Methods**

178 **Sample Collection**

179 *Montipora digitata* colonies were collected from Hazard Bay (S18°38.069', E146°29.781') and
180 Pioneer Bay (S18°36.625', E146°29.430') at Orpheus Island two days before the full moon on the
181 29th of March 2018 and brought to the National Sea Simulator (Seasim) at the Australian Institute
182 of Marine Sciences (AIMS) (Permit number: G12/35236.1). To minimize the collection of clonal
183 *M. digitata* fragments, colonies were collected a minimum of 5-10 m apart laterally along the
184 shore, given that clones tend to propagate shoreward with wave action (Heyward, pers. comm).
185 Upon arrival to the Seasim, colonies were placed in outdoor tanks that were fed with 27.5°C
186 filtered seawater and sorted into either the “Fat-finger” or “yellow-spathulate” morphs (Stobart,
187 2000).

188 **Spawning and fertilization design**

189 Colonies were monitored for spawning starting 2 nights before the full moon (29th of
190 March) starting around dusk. Bundles were collected on the 6th of March, 6 nights past the full
191 moon (31st of March 2018). Egg-sperm bundles were collected from multiple colonies (listed
192 below) and separated using 60 µm mesh filters. Sperm was set aside, and eggs were washed again
193 3x in 60 µm mesh in 0.2 µm filtered seawater (hereafter FSW). Two types of reproductive crosses
194 were generated. Individual crosses were produced following a diallel design using roughly equal
195 numbers of eggs and a sperm concentration of 10⁶/ml. A bulk culture was also produced by mixing
196 eggs and sperm from multiple colonies together (eggs from parents Ytag1, A, Z1, D, C, D4, Ytag2,
197 C3, A1, D5, D2, C1 and sperm from Yag1 Z3, C2, WT3, C3, Y2, H, C1, A, C, D4). Gametes were
198 monitored for cell division and when successful cell division was observed, embryos were washed
199 3x in 0.2 µm FSW to remove residual sperm and maintained at a density of ~1 larvae/mL in
200 individual culture tanks with constant flow through of 27.5°C FSW. The bulk culture was reared
201 in a single 500L tank with 27.5°C FSW. Simultaneously, three crosses from four parental colonies
202 (hereafter larval families) were reared in individual 45 L tanks with flow through 27.5°C FSW.
203 Following spawning, tissue biopsies from contributing parents were preserved in 100% EtOH and
204 stored at -20°C for DNA extraction and ITS2 amplicon sequencing.

205 **Larval thermal stress experiment**

206 At four days post-fertilization, individual larvae from each cross (HxWT3, WT3xC1,
207 H1xWT3) and the bulk culture were placed into individual wells of sterile 48-well plates pre-filled
208 with FSW (Corning[®], Sigma-Aldrich[®]). Plates were sealed into individual transparent plastic bags
209 to prevent evaporation and placed into temperature and light controlled incubators set at 27°C and

210 32°C. Light was set at 60 PAR ($\mu\text{mol m}^{-2} \text{s}^{-1}$) (Sylvania FHO24W/T5/865 fluorescent tubes)
211 with a 14:10 light:dark cycle. For the bulk culture, four replicate plates were placed at each
212 temperature, each with 48 larvae ($n = 192$ larvae at 27°C and 32°C each). For the individual
213 crosses, three replicate plates with two rows per cross per plate were placed at each temperature
214 ($n = 16$ larvae/plate $\times 3 = 48$ larvae at 27°C and 32°C per cross). At the time of well-plate stocking,
215 a subset of different individual larvae from both the bulk culture and individual crosses were
216 preserved in 100% EtOH and stored at -20°C for DNA extraction and ITS2 amplicon sequencing.
217 The experiment continued for two months with periodic screening of larvae for survival and
218 collection of non-invasive physiological data. The experiment was terminated when survival at
219 32°C reached an average of 50% across all treatments to ensure sufficient remaining biomass for
220 analysis of symbiont community composition. Surviving larvae were individually preserved in
221 100% EtOH and stored at -20°C for DNA extraction and amplicon sequencing.

222 **Juvenile thermal stress experiment**

223 At four days post-fertilization, additional larvae from both the bulk culture and individual
224 crosses were placed into sterile 6-well plates (Corning®, Sigma-Aldrich®) pre-filled with FSW. A
225 small chip (1mm^2) of coral rubble was added to each well as a settlement inducer. Larvae were
226 allowed to settle overnight followed by a complete water change. Due to high variability in
227 settlement success, only bulk culture larvae settled into juveniles in high enough numbers for
228 adequate replication in the subsequent thermal stress experiments. As with the larval experiment,
229 the 6-well plates were individually wrapped in plastic bags and placed into temperature and light
230 incubators under the same conditions described above. The experiment continued for 20 days with
231 periodic monitoring of juveniles for survival and collection of non-invasive physiological data.
232 The experiment was then terminated when survival at 32°C reached an average of 50%, and
233 samples were preserved as described for larvae.

234 **Physiological Data**

235 Larval survival was scored from 19 April 2018 to 15 June 2018 over 21 timepoints from 0
236 to 1,360 hours after the experimental start. Juvenile survival was scored from 31 May 2018 to 20
237 June 2018 over 3 timepoints. Larvae were deemed dead when they were not seen inside the well.
238 A juvenile was deemed dead when tissue was not present and only skeleton remained.

239 Larval size was measured on 23 May 2018, between 718 and 936 hours from the
240 experiment start (timepoints 17 and 18). To measure size, wells were visualized under a dissecting
241 microscope (Zeiss) and a still image was captured when larvae were in a lateral position.

242 Microscopy Pulse Amplitude Modulated fluorometry (Microscopy PAM, Waltz) was used
243 to assess the photosynthetic performance and functioning of symbionts within individual *M.*
244 *digitata* larvae and juveniles. Specifically, effective photosystem II quantum yield ($Y_{II} = F_m'/F_m -$
245 $F)/F_m'$) was measured at two timepoints: 400 and 1,269 hours. ImagingWin software (v2.46x6)
246 was used with the following settings: Measuring light (Intensity 6, Frequency 8), Actinic light
247 (Intensity 3), Gain and Damping (both 2). Individual larvae were outlined as the area of interest
248 (AOI). Two replicate larvae per plate for 3x replicate plates were measured ($n = 6$ larvae per cross
249 per treatment per timepoint).

250 **Statistical Analysis of Physiological Data**

251 Physiological data was modeled as a function of temperature treatment within crosses using
252 R (v. 4.1). For all models, assumptions of homogeneity of variance, linearity, normality and
253 autocorrelation were checked, and tests modified where appropriate. The presence (1) or absence
254 (0) of larvae and juveniles at each monitoring time-point was used as input for a survival analysis
255 using the ‘Survminer’ package. Survival over time was modeled as a function of temperature
256 treatment and cross type. Significance of factors was assessed using a Generalized Linear model
257 using a binary (logit) distribution. Larval size was modelled as a function of length and temperature
258 treatment with a random effect of their well plate environment using the model
259 (Length~Treatment, random=~1|Plate, data = larvae_size, na.action = na.exclude) in the “lme”
260 package. For the PAM fluorometry data, linear mixed models were fit for each timepoint using the
261 package ‘nlme’ to test for significant differences in YII due to temperature treatment (categorical
262 factor) and replicate plate (random factor). The main effect of temperature was determined using
263 Type II Analysis of Deviance tests using the ‘car’ package. The assumption of homogeneity of
264 variance was violated for PAM values originating from the bulk culture larvae at 1,360 hours,
265 therefore a generalized least squares model (GLS) was implemented using the ‘nlme’ package,
266 including an ARMA correlation structure (“plate”) with categorical weights (VarInd) for
267 temperature treatment, fit by maximizing the restricted log-likelihood (REML).

268 **DNA extraction, Preparation of ITS2 Amplicon Libraries and Sequencing**

269 DNA was extracted from adult biopsies, skeletal debris, and individual larvae and juveniles
270 using modified SDS protocol outlined here (Quigley et al. 2017). The Symbiodiniaceae ITS2
271 region was amplified using the SYM_VAR_5.8S2 (forward: 5’-
272 GTGACCTATGAACTCAGGAGTCGAATTGCAGAACTCCGTGAACC-3’) and
273 SYM_VAR_REV (reverse: 5’-
274 CTGAGACTTGCACATCGCAGCCGGGTTWCCTTGTYTGACTTCATGC-3’) primers
275 following the protocol described in (Hume et al. 2019). Most PCR reactions contained: 0.5µl of
276 equimolar (10mM) dNTPs, 5 µl 5X Q5 PCR buffer (New England Bio Labs), 0.25 µl Q5 DNA
277 polymerase (New England Bio Labs), 2 µl DNA (20ng/µl) template, 0.25 µl of each primer (10
278 µM), 0.25 µl BSA (20 mg/µl) (New England Bio Labs), and 16.5 µl Milli-Q ultrapure water per
279 reaction. However some samples with limited DNA were amplified at 1ul DNA with an adjusted
280 amount of 17.5ul Milli-Q ultrapure water per reaction). The amplification profile included an
281 initial denaturation step of 98°C for 30 sec with cycles of 98°C for 10 sec, 56°C for 1 min, and
282 72°C for 30 sec, with a final elongation step of 72°C for 5 min. Samples were amplified to the
283 lowest cycle number at which a band was first observed ([Table S1](#)). Twelve samples failed to
284 amplify and were discarded from subsequent steps. Water was used as a negative control during
285 PCR and only samples from reactions where no negative control bands were observed were carried
286 forward for sequencing. In a second six cycle PCR, Illumina primers with custom dual index
287 barcodes were incorporated. Barcoding PCR reactions contained: 0.5µl of equimolar (10mM)
288 dNTPs, 5 µl 5X Q5 PCR buffer (New England Bio Labs), 0.25 µl Q5 DNA polymerase (New
289 England Bio Labs), 3 µl DNA template, 1 µl of each of two barcodes (10 µM), 0.25 µl BSA (20
290 mg/µl) (New England Bio Labs), and 14 µl Milli-Q Ultrapure water per reaction. The amplification
291 profile for barcoding contained an initial denaturation step of 98°C for 30 sec and six cycles of
292 98°C for 10 sec, 59°C for 1 min, and 72°C for 30 sec, with a final elongation step of 72°C for 2

293 min. Barcoded amplifications were cleaned using a SPRI bead based size selection protocol
294 (Beckman Coulter) with a 0.65:1 bead to sample ratio to select for nucleic acid sequences between
295 300 and 400 bp in length, which corresponds with target Symbiodiniaceae ITS2 band sizes (Hume
296 et al. 2019). Following bead clean up and size selection samples were pooled in groups of 4-10
297 based on visual assessment of gel band intensity, and a 1:100 dilution of each sample pool was
298 qPCR amplified (Aria MX, Agilent) using the Illumina i5 and i7 sequencing primers to quantify
299 the relative abundance of each sample for subsequent pooling. qPCR reactions were run in
300 duplicate. Pools were then mixed in equimolar volumes, and the final library was sequenced at the
301 USC NCCC Molecular Genomics Core on the Miseq V2 sequencing platform (PE 250). Samples
302 with insufficient read depth (N=36, < 1000 reads per sample) were subject to two rounds of
303 additional amplification, barcoding, size selection and sequencing to increase read yields ([Table](#)
304 [S1](#)). Additional samples with sufficient read depth in the first sequencing run were also re-
305 amplified to serve as internal controls for composition and relative abundance of ITS2 amplicons
306 across independent runs. High similarity was evident within internal control samples across
307 sequencing runs ([Figure S1](#)), justifying concatenation of raw reads from individual runs by sample
308 prior to statistical analyses.

309 **Assigning taxonomy**

310 A hybrid Symportal-DADA2 approach was used to delineate and taxonomically identify
311 sequence variants. An important attribute of Symportal is that it measures symbiont abundance
312 based on the formation of ITS2 profiles that correspond to “defining intragenomic variants” (DIVs)
313 from the family Symbiodiniaceae (Hume et al. 2019). This assignment accounts for potential
314 overinflation of diversity metrics by adjusting for intragenomic variation of ITS2 Amplicon
315 Sequence Variant (ASVs) using patterns of co-occurrence across samples (Hume et al. 2019).
316 However, given the high relatedness of our sample set, co-occurrence more likely results from the
317 biological mechanism of shared inheritance. The Symportal pipeline also discards background
318 symbiont types, defined as those sequences that are represented by ≤ 200 reads. However,
319 Symportal does not account for repeated or paired measures, and is therefore susceptible to missing
320 background variants present initially in low abundance but increasing in abundance in time-series
321 sample sets. Therefore, to understand whether rare variants with increased abundance in heat-
322 treated samples were also present in control and pre-stress conditions regardless of their absolute
323 threshold abundances in addition to correcting for the presence of intragenomic variation when
324 assessing community diversity, Symportal DIVs and taxonomies were overlaid onto DADA2
325 ASVs. To do this, a Symportal analysis was used to generate a taxonomy database specific to this
326 dataset and to identify similar co-occurring sequences that comprise representative DIVs. DADA2
327 was then run on the same raw read dataset to generate ASVs that were then assigned sequence and
328 DIV identities based on the Symportal taxonomy. This approach also allowed us to retain
329 background-low abundance reads while also accounting for intragenomic variation of ITS2 using
330 the Symportal framework as described in greater detail below.

331 Amplicon sequencing of the ITS2 region was undertaken across 120 samples with 90
332 samples successfully resulting in 4.76×10^6 raw reads. These reads were processed by Symportal
333 with default parameters (“--analyse” with “--num_proc 3”). This yielded a DIV matrix and
334 taxonomy assignments for each sample based on the Symportal database. The taxonomy database
335 from this run was used to generate a Phyloseq data bin for downstream analysis.

336 In parallel, the same reads were trimmed of their Illumina adaptors using bbdduk (Bushnell
337 2020), and their barcodes using cutadapt (Martin 2011) (Table S2). These reads were then filtered
338 and processed using DADA2, resulting in a total of 4.08×10^6 trimmed reads (Callahan et al. 2016).
339 A total of 81 of 90 samples passed the trimming and filtering steps in DADA2. The heat treated
340 larval family samples were lost in this processing due to poor quality reads (Table S2). An ASV
341 table was generated using the standard DADA2 protocol for ITS amplicon sequencing reads
342 (Callahan et al. 2016). Taxonomy was assigned to ASVs by using the Symportal database specific
343 to this dataset as described above to ensure a 1:1 correspondence. ASVs were then collapsed into
344 DIVs by summing counts across individual ASVs comprising the DIV using the multisequence
345 ITS2-profile types identified by Symportal. Rare ASVs (those originally discarded by Symportal)
346 were retained as individual columns in the matrix. For example, in our dataset there were four
347 *Cladocopium* ASVs that formed four unique and overlapping ITS2 DIV profiles, “C15”, “C15-
348 C15dq”, “C15-C15dq-C15dr” and “C15-C15dq-C15dr-C_1365”. For samples that Symportal
349 identified as having “C15” or “C15-C15dq” as their dominant DIV, the DADA2 ASV matrix was
350 modified to create a new column which was the sum of all C15 ASVs or all C15 plus C15dq ASVs,
351 effectively replacing the individual ASV columns with the DIV. The majority of samples had
352 “C15-C15dq-C15dr-C_1365” as their dominant DIV. Counts for samples that exhibited a C15 or
353 C15+C15dq DIV but still had individual counts for C15dq or C15dr were also maintained in the
354 sequence matrix. (Table S3).

355 Alpha and Beta Diversity

356 The Shannon Diversity Index was calculated in Phyloseq (McMurdie and Holmes 2013)
357 as a metric of alpha diversity for each sample. Shannon diversity was then modelled as a function
358 of temperature treatment (bulk culture larvae and juveniles) or larval family using beta regression
359 (Cribari-Neto and Zeileis 2010) to be able to properly fit continuous values between 0-1. For
360 families, pre-stress and ambient larvae were grouped together. Pairwise comparisons among means
361 with respect to factor levels (pre-stress, ambient, and heat, or larval family) were conducted using
362 Tukey’s HSD, adjusting p-values for multiple comparisons. Beta diversity was visualized using
363 nonmetric multidimensional scaling (NMDS) with a Bray-Curtis distance implemented in
364 Phyloseq for bulk culture larvae and juveniles and larval families (McMurdie and Holmes 2013).
365 Following NMDS scaling of symbiont communities, evenness of dispersion across bulk culture
366 larvae and juveniles and larval families were evaluated using the betadisper function in the vegan
367 package (Oksanen et al. 2007). Only bulk juvenile samples satisfied assumptions for parametric
368 testing (Table S4) and a PERMANOVA was used to test the effect of treatment on community
369 differences using the adonis2 function. A non-parametric test implemented with the anosim
370 function was used to test the effect of treatment (bulk culture larvae) or family on beta community
371 differences (Oksanen et al. 2007).

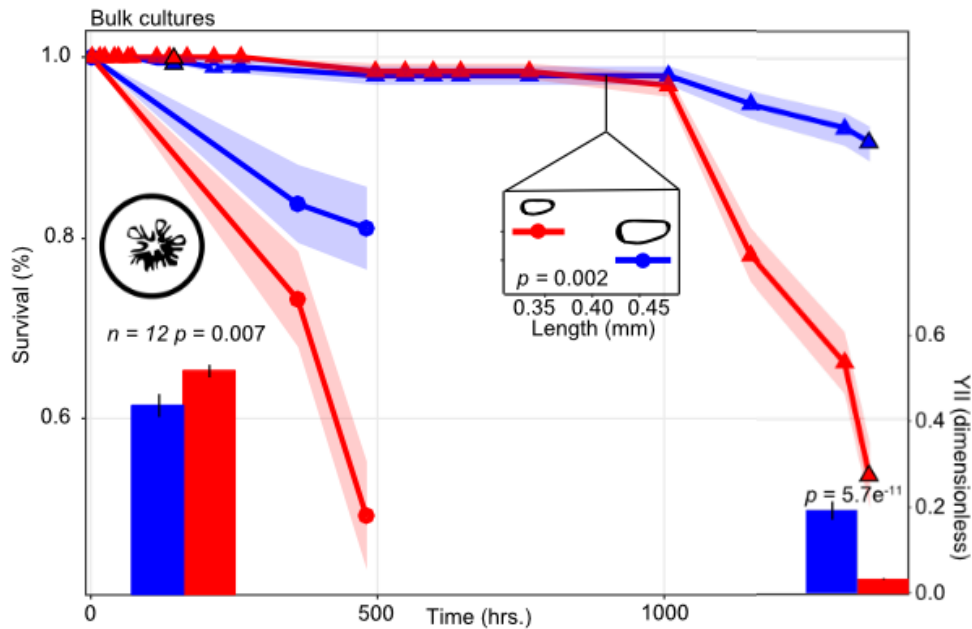
372 Results

373 1. Fitness related traits vary with temperature in larvae and juveniles

374 Larvae and juveniles produced from bulk culture fertilizations survived significantly better
375 at 27°C compared to those exposed to 32°C (Fig. 1, Kaplan-Meier survival, $p < 0.0001$ and
376 0.00014, respectively). Compared to larvae, juveniles exhibited a higher susceptibility with a mean

377 survival of ~475 hours, whereas larvae did not reach a mean of 50% survival until ~1,360 hours
 378 of exposure to 32°C (Fig. 1, [Figure S2](#)).

379 Larvae produced from bulk culture fertilizations were significantly smaller at 32°C (0.45
 380 mm ± 0.03) compared to those at 27°C (0.34 mm ± 0.03) after 814 hrs of heating (LRT, df = 1, p
 381 = 0.002, Fig. 1 inset). After 400 hrs at temperature, bulk larvae at 32°C had significantly higher
 382 photosynthetic yields relative to larvae at 27°C (p = 0.007). This was reversed after 1,269 hrs, in
 383 which larvae at 27°C had significantly higher yields (p = $5.7e^{-11}$).



384
 385 **Figure 1.** Survival, size and photosynthetic efficiency of ambient and heat-treated bulk culture
 386 larvae and juveniles. Lines indicate the percent survival (left axis) of larvae (triangles) and juvenile
 387 (circles) as a function of treatment (red: heat, blue: ambient). Shading indicates the 95% confidence
 388 interval. Differences in the size of ambient and heat exposed bulk culture larvae were quantified
 389 at one time point and are shown as the mean ± standard error as a function of treatment in the upper
 390 inset. Photosynthetic efficiency (YII, right axis) of larvae was measured at two timepoints.

391 2. Fitness related traits vary among larval families

392 Larval survival was impacted by family origin (HxWT3, WT3xC1 and Z3xWT3, Fig. 2).
 393 Specifically, larvae from family Z3xWT3 survived significantly better at both temperatures
 394 compared to larvae from family WT3xC1 (Kaplan-Meier survival – KM, p = 0.042 and 0.025).
 395 Larvae from HxWT3 survived significantly better compared to WT3xC1 larvae at 27°C but not
 396 32°C (KM, p = 0.045 and 0.18) but survival was similar to Z3xWT3 at both temperatures (KM, p
 397 = 0.97 and 0.35). Hence, at 32°C, survival of larvae was highest overall in the family Z3xWT3,
 398 followed by HxWT3 and WT3xC1 (Fig. 3). Larval survival from the three crosses was not
 399 significantly different at 27°C compared to 32°C after 1360 hours of heating (Kaplan-Meier
 400 survival, p = 0.12, 0.4, and 0.5, for HxWT3, WT3xC1 and Z3xWT3, respectively, Fig. 2, 3, [Figure](#)
 401 [S2](#)).

402 On average, effective quantum yield of photosystem II (YII) in larval families ranged from
403 0.49 ± 0.1 to 0.03 ± 0.009 . YII varied significantly at both 400 and 1269 hrs between temperature
404 treatments for all families except HxWT3. Specifically, YII values measured in larvae from
405 families HxWT3, WT3xC1 and Z3xWT3 were all significantly greater at 27°C ($0.2 \pm 0.08 - 0.13$
406 ± 0.06) compared to 32°C ($0.04 \pm 0.01 - 0.03 \pm 0.008$) after 1269 hrs of heating (Likelihood Ratio
407 Test-LRT, $df = 1$, $p = 2.9e^{-08}$, $8.3e^{-05}$, $5.9e^{-05}$, respectively, Fig. 2A-C). In family WT3xC1, YII
408 values were significantly greater in larvae at 27°C compared to 32°C ($0.4 \pm 0.03 - 0.38 \pm 0.05$,
409 LRT, $df = 1$, $p = 0.008$) following 400 hrs of exposure, although the opposite trend was found in
410 Z3xWT3 ($0.3 \pm 0.1 - 0.5 \pm 0.1$, LRT, $df = 1$, $p = 0.003$). Similar to the bulk culture (Fig. 1), larvae
411 from family Z3xWT3 exhibited significantly higher YII at 32°C (0.52 ± 0.01) compared to those
412 at 27°C (0.44 ± 0.03) after 400 hrs of heating (LRT, $df = 1$, $p = 0.007$). After 1360 hrs, this trend
413 was significantly reversed (0.19 ± 0.02 versus 0.03 ± 0.002 , Generalized Least Squares - GLS, df
414 $= 1$, $p = 5.7e^{-11}$).

415 Larval size also varied across the three families at 27°C, in which HxWT3 larvae were the
416 largest (0.49 ± 0.06 mm, Fig. 2A). After 814 hrs of heating at 32°C, larvae from all families were
417 smaller, although only larvae from family HxWT3 were significantly smaller than their paired
418 controls (0.32 ± 0.02 mm length; $n = 6$, LRT, $df = 1$, $p = 0.003$, Fig. 2A). Larvae from the family
419 WT3xC1 were the smallest after heating (0.28 ± 0.03 mm compared to $0.34 \pm .05$, LRT, $df = 1$, p
420 $= 0.18$). The decrease in larval size under heat was less in family Z3xWT3 (32°C: 0.35 ± 0.04 mm,
421 27°C: 0.42 ± 0.06 , LRT, $df = 1$, $p = 0.09$).

422

423

424

425

426

427

428

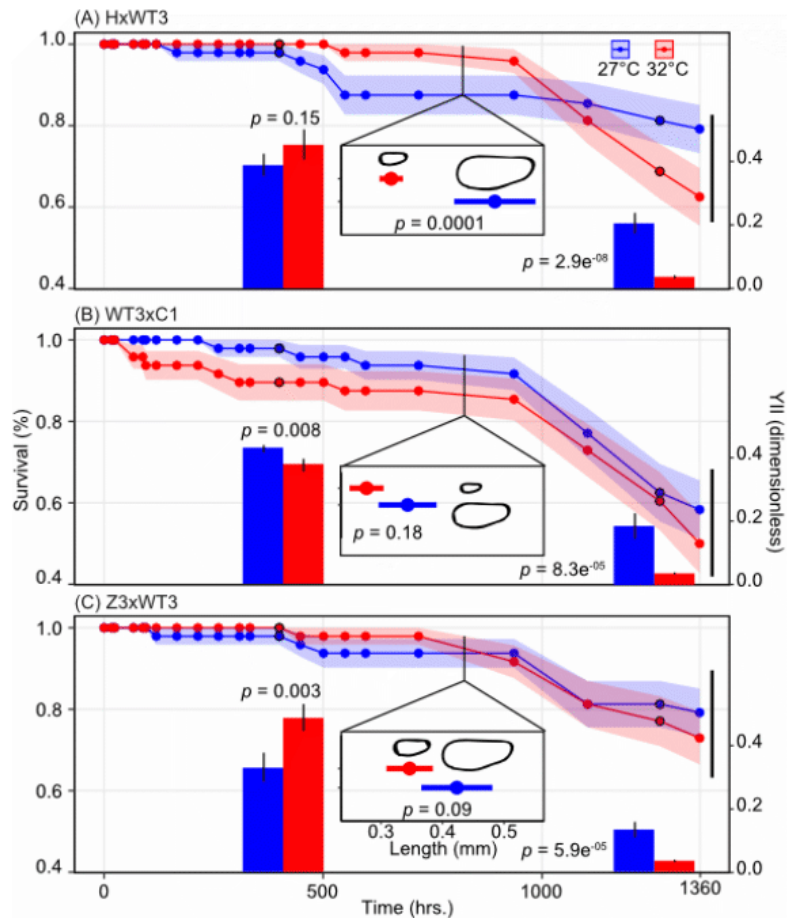
429

430

431

432

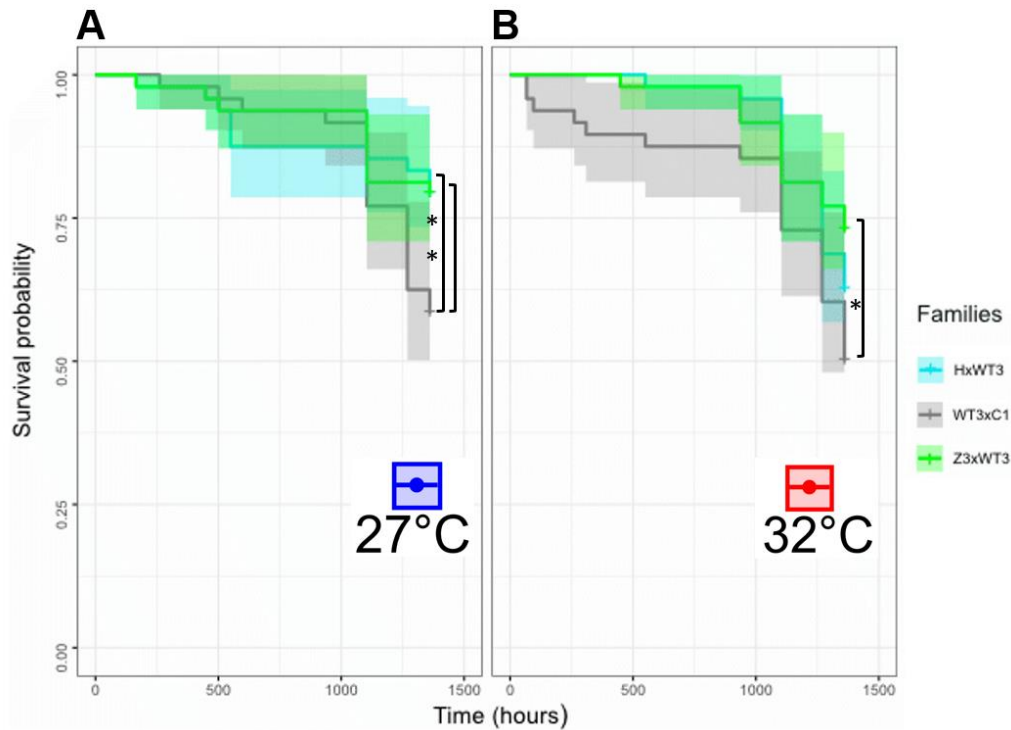
433



434

435 **Figure 2.** Survival, size and photosynthetic efficiency of ambient and heat-treated larvae derived
 436 from crosses between adults (A) HxWT3, (B) WT3xC1, and (C) Z3xWT3. Within panels A-C
 437 lines indicate the percent survival (left axis) of larvae as a function of treatment (red: heat, blue:
 438 ambient control). Shading indicates the 95% confidence interval. Differences in the size of ambient
 439 and heat-treated larvae were quantified at one time point and are shown as the mean \pm standard
 440 error as a function of treatment in the central insets. Photosynthetic efficiency (right axis) was
 441 measured at two timepoints.

442



443

444 **Figure 3.** Survival probabilities of ambient and heat-treated larvae from crosses between adults
 445 HxWT3 (light blue), WT3xC1 (grey), and Z3xWT3 (light green). A. Survival probabilities for
 446 family comparisons HxWT3 and WT3xC1 and Z3xWT3 and WT3xC1 were significantly different
 447 in ambient conditions ($p = 0.045$, $p = 0.042$, respectively). B. Survival probabilities for family
 448 comparisons Z3xWT3 and WT3xC1 were significantly different in heat-treated conditions ($p =$
 449 0.025).

450 3. Symbiont communities differ in larvae, but not juveniles exposed to heat stress

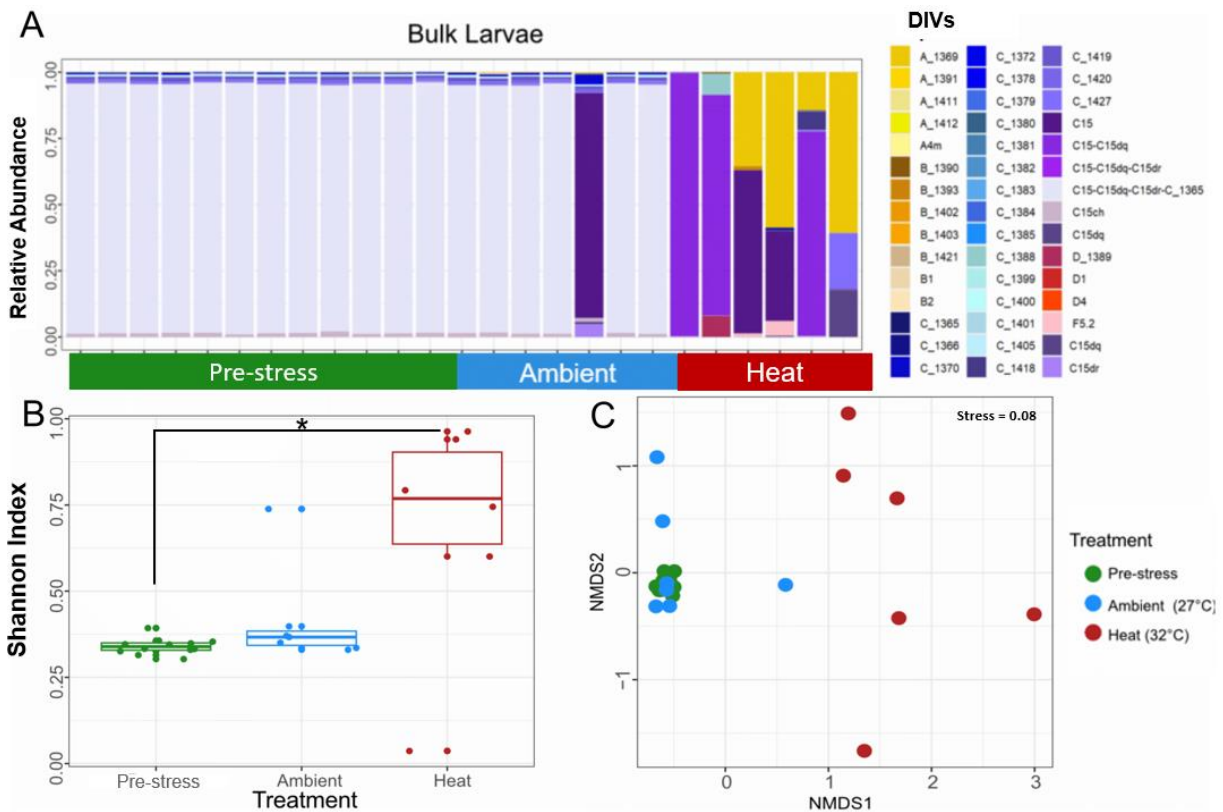
451 Symbiodiniaceae communities' larvae produced from bulk culture fertilizations did not
 452 vary between 27°C and the pre-experimental timepoint (or pre-stress). These larvae were
 453 dominated by the ITS2 DIV profile C15-C15dq-C15dr-C_1365 and low abundances (< 5%) of
 454 *Symbiodinium* spp. were also detected (Fig. 4A, [Figures S4-S5](#)). Larvae from the 32°C treatment
 455 showed a markedly different symbiont community compared to larvae at 27°C. This difference
 456 included both a change in the dominant C15 ITS2 DIV profile as well as notable changes in relative
 457 abundance of *Symbiodinium* spp., *Breviolum* spp., *Dursudinium* spp., and *Fugacium* spp. in
 458 addition to other *Cladocopium* spp. variants (Fig. 4A).

459 Shannon diversity, which in this case describes the number and relative abundance of algal
 460 DIVs within an individual larva (Peet 1974), also confirmed the shift in community composition
 461 within heat-treated larvae compared to pre-stress samples (Pairwise comparisons between pre-
 462 stress and 32°C, $p = 0.0033$, Fig. 4B, [Table S5](#)). A similar trend evident between heat and ambient
 463 treatments (Pairwise comparisons between 27°C and 32°C, $p = 0.0535$, Fig. 4B, [Table S2](#)). Beta
 464 diversity, which describes differences in symbiont community composition among larval samples,
 465 also distinguished heat-treated larvae from ambient and pre-stress samples (NMDS with Bray-
 466 Curtis distance, Fig. 4C, [Table S6](#)). Additional testing of dispersion between beta diversity

467 community values revealed a significant effect of treatment on larval community composition
 468 (BETADISPER $p < 0.001$, ANOSIM, $R = 0.48$ and $Sig = 0.001$, [Table S7](#)).

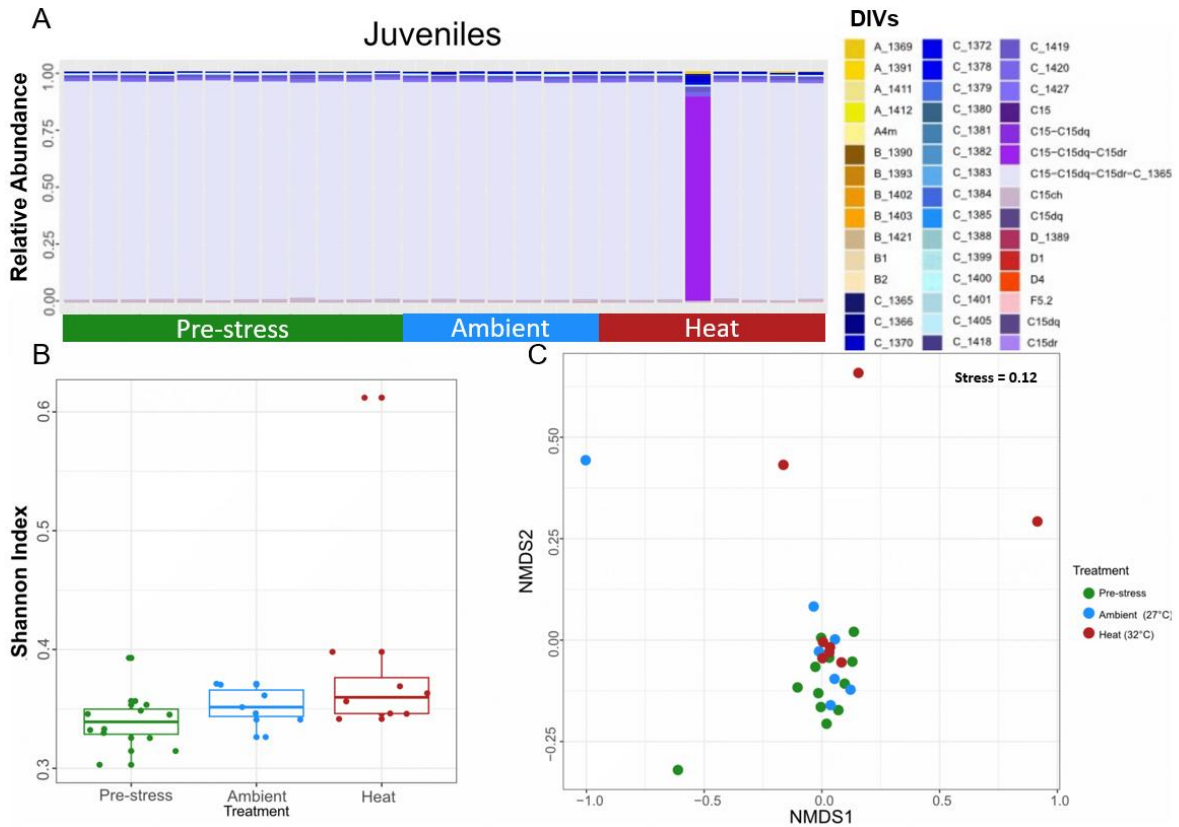
469 This pattern was not evident in juveniles derived from the same bulk culture fertilization
 470 and exposed to a similar heat stress. Juveniles remained dominated by the same C15-C15dq-
 471 C15dr-C_1365 DIV regardless of treatment (Fig. 5). Although some heat-treated juveniles
 472 showed increases in *Symbiodinium* spp. and *Breviolum* spp. variants in comparison to ambient
 473 controls and pre-stress larvae, no difference in alpha diversity was detected between ambient and
 474 heat treatments (Pairwise comparisons between 27°C and 32°C $p = 0.29$, Fig. 5A,B, [Table S5](#)).
 475 Although a similar trend was detected between pre-stress larvae and heat treated juveniles as was
 476 observed between ambient and heat treated larvae (Pairwise comparisons between pre-stress
 477 larvae and 32°C, $p = 0.059$, Fig. 5B, [Table S5](#)). Visualizing beta diversity using NMDS with
 478 Bray-Curtis distance confirmed no major differences in symbiont communities between the pre-
 479 stress, ambient and heat-treated juvenile samples (Fig. 5C). Nor was a significant effect of
 480 treatment detected on beta community dispersion (BETADISPER $p = 0.946$, PERMANOVA p
 481 $= 0.385$, [Table S8](#)).

482



483 **Figure 4.** Symbiont community composition in bulk larval cultures. (A) Barplots showing
 484 relative abundance of Symbiodiniaceae DIVs from pre-stress (green), ambient (27°C, blue) and
 485 heat (32°C, red) treated bulk larvae. (B) Boxplot distributions of Shannon Alpha diversity in pre-
 486 stress, ambient (27°C) and heat (32°C) treated larvae. The asterisks indicate significant pairwise
 487 differences between pre-stress (green) and heat (32°C, red) treatment (* $p < 0.05$). (C) Beta
 488

489 diversity of symbiont communities in pre-stress, ambient and heat-treated bulk larvae visualized
 490 using an NMDS plot with Bray-Curtis distance (Stress = 0.08).



491
 492 **Figure 5.** Symbiont community composition in juveniles produced from bulk cultures. (A)
 493 Barplot showing relative abundance of Symbiodiniaceae DIVs in pre-stress (green), ambient
 494 (27°C, blue) and heat (32°C, red) treated juveniles. (B) Boxplot distributions of Shannon Alpha
 495 diversity in pre-stress, ambient (27°C) and heat (32°C) treated juveniles. (C) Beta diversity of
 496 pre-stress larvae, ambient and heat-treated juveniles visualized using an NMDS plot with Bray-
 497 Curtis distance (Stress = 0.12).

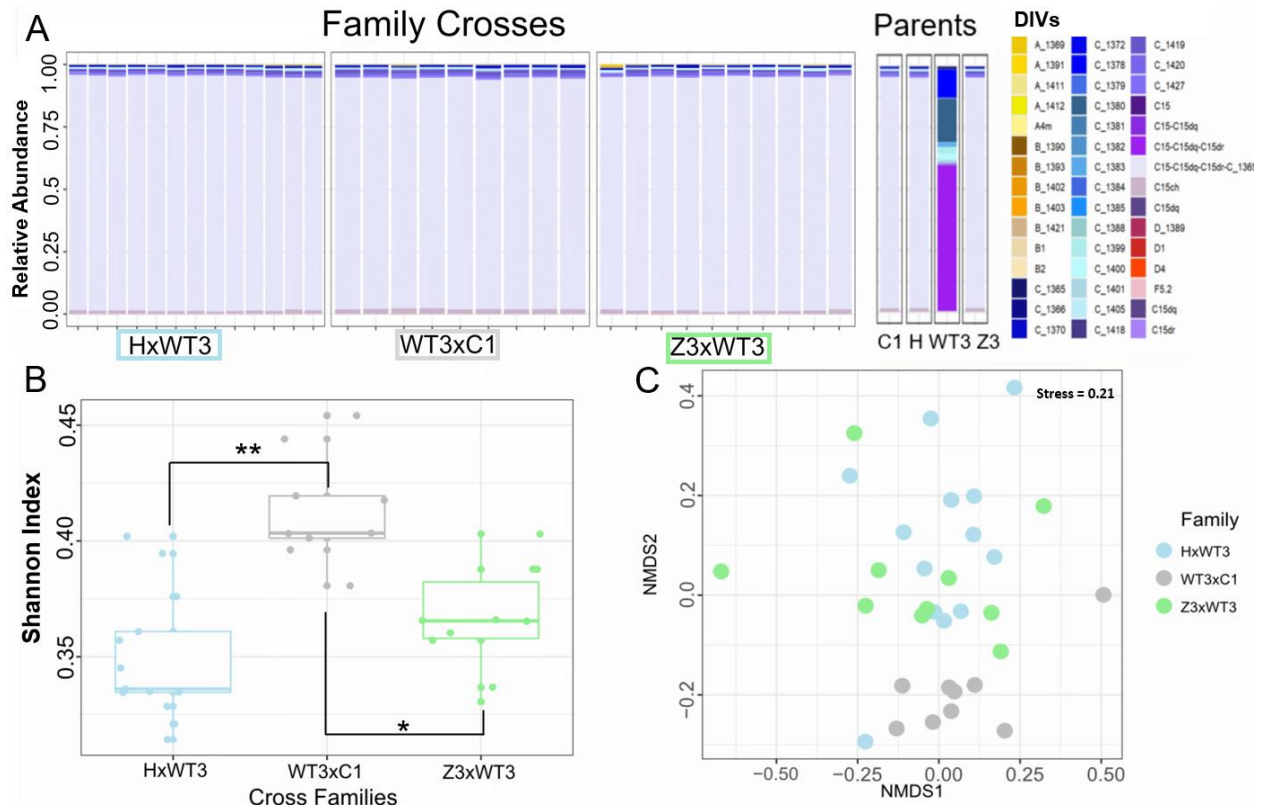
498 **4. Targeted reproductive crosses reveal distinct symbiont communities in mothers are**
 499 **reflected in offspring**

500 Only larvae from the 27°C treatment yielded successful amplification, restricting
 501 comparisons to differences among families in the ambient treatment. Larvae from all three crosses
 502 were dominated by the same *Cladocopium* spp. DIV (C15-C15dq-C15dr-C_1365). Background
 503 taxa, or those present at <5% abundance, exhibited a DIV profile that was similar to the bulk
 504 culture larvae at 27°C (Fig. 6A, 4A). Parental colonies were similarly dominated by DIV C15-
 505 C15dq-C15dr-C_1365, except for colony “WT3”, which was dominated by *Cladocopium* profile
 506 C15-C15dq-C15dr (Fig. 6A).

507 Alpha diversity was significantly higher in family WT3xC1 in comparison to the other
 508 crosses (HxWT3 – WT3xC1, *padj* < 0.0001 and WT3xC1 – Z3xWT3, *padj* = 0.0001, Fig. 6B).

509 This pattern was also reflected in beta diversity (NMDS with Bray-Curtis distance, BETADISPER
 510 $p = 0.017$, Anosim, $R = 0.17$ and $Sig = 0.006$, [Table S9](#)). Specifically, larvae from cross WT3xC1
 511 clustered strongly together, likely driven by low-abundance DIV profiles, whereas the other
 512 crosses were more evenly distributed across the ordination space (Fig. 6C, [Table S6](#)).

513
 514



515

516 **Figure 6.** Symbiont community composition in larval crosses and their parents in control
 517 conditions. (A) Barplot showing relative abundance of Symbiodiniaceae DIVs in individual
 518 larvae grouped by family (notation: dam x sire). Symbiodiniaceae DIVs of parent coral are
 519 shown in an additional panel. (B) Boxplot distributions of Shannon Alpha diversity. Asterisks
 520 indicate significant pairwise differences between family pairs, Z3xWT3 and WT3xC1
 521 ($*padj=0.0001$), and HxWT3 and WT3xC1 ($**padj<0.0001$). (C) Beta diversity of symbiont
 522 communities by family visualized using an NMDS plot with Bray-Curtis distance (Stress =
 523 0.21).

524

525 **Discussion**

526 In this study we showed changes in symbiont communities in the early life-history stages
527 of a common, vertically transmitting coral, *Montipora digitata*, in response to heat stress.
528 Specifically, under heat stress, we found symbiont communities differed between temperature
529 treatments in larvae but detected no differences in juveniles derived from the same bulk culture
530 fertilization. Although we cannot confirm whether these changes in larvae are due to an active (i.e.
531 shuffling) or passive (i.e. increase in opportunistic symbionts or last symbiont standing)
532 mechanism, we did observe significant differences in survival duration between larvae and
533 juveniles, with larvae surviving more than twice as long as juveniles. Moreover, symbiont
534 communities in heat-treated larvae became dominated by representatives of canonically stress-
535 tolerant genera. Finally, we also show that increased maternal diversity is reflected in offspring.
536 Overall, our results indicate larvae can survive twice as long when compared to juveniles under
537 the same warming conditions, potentially driven by symbiont shuffling, suggesting that the
538 juvenile life stage is more at risk from climate warming.

539 **Life stage specific differences in physiology and symbiont community diversity in response** 540 **to thermal stress**

541 Both larvae and juveniles were dominated by the same C15 DIV, but larvae survived much
542 longer on average and their symbiont community composition showed greater differences under
543 heat treatment than juveniles. There is ample evidence to show that symbiont communities drive
544 host physiology in coral adults (Quigley et al. 2022, 2023; Terrell et al. 2023), underpinned by
545 differences in symbiont tolerance to stress (Swain et al. 2021). *Symbiodinium microadriaticum*
546 and *Durusdinium trenchii*, for example, tend to produce less reactive oxygen species (ROS), a
547 molecular response associated with coral bleaching, when exposed to heat stress compared to
548 *Breviolum minutum* and *Cladocopium goreaui*, (Lesser 2019). Additionally, these dynamics within
549 a host can start as early as gametogenesis in vertically transmitting species, as changes in symbiont
550 communities within oocytes were detected in a mass bleaching year (Quigley et al. 2019). Taken
551 together, we postulate that the altered symbiont community in larvae may have afforded them a
552 fitness advantage which then allowed them to persist longer under thermal stress. Assuming the
553 community shift led to gains in heat tolerance, this suggests that either the maternal colonies or
554 the larvae may be actively re-arranging their symbiont communities as an acclimatization
555 mechanism to cope with heat stress. This mechanism has been seen in adults (Berkelmans and van
556 Oppen 2006), eggs of vertical transmitters (Quigley et al. 2019), and the juveniles of some coral
557 species (Terrell et al. 2023). The increased relative abundance of symbionts from the genera
558 *Symbiodinium*, *Durusdinium* and *Fugacium* further supports this conjecture, as these are among
559 the most stress tolerant genera (Swain et al. 2017). Therefore, these changes in the symbiont
560 community could be described as adaptive shuffling; however, we cannot conclusively determine
561 if these changes preceded differential mortality and are thus indicative of it.

562 Alternatively, larvae may be more robust compared to juveniles for reasons unrelated to
563 symbionts. Larvae may be more resistant because of their positive buoyancy from high lipid
564 content early in life, which exposes them to harsh environmental conditions such as high ultraviolet
565 radiation and temperature at the sea surface (Glynn 1993; Wellington and Fitt 2003; Rodriguez-
566 Lanetty et al. 2009; Aranda et al. 2011; Gleason and Hofmann 2011). Moreover, during the motile
567 larval stage, they are actively exposed to both surface and benthic conditions from several days to
568 multiple weeks (Ritson-Williams et al. 2009), forcing them to withstand highly variable
569 environmental conditions. Metamorphosis is also an energetically costly process that depletes

570 larval energy reserves and may result in more susceptible juvenile stages (Edmunds et al. 2001;
571 Ritson-Williams et al. 2009). The enhanced survival of the larvae compared to juveniles under
572 heat stress may therefore result from either or both the change in symbiont community and the
573 overall robustness of larvae. In summary, we hypothesize that lower survival of juveniles may be
574 driven by lack of an ability to adjust symbiont communities combined with diminished energetic
575 reserves post-metamorphosis, suggesting the juvenile stage may be the most susceptible life-
576 history stage for corals.

577 Interestingly, we found Symbiodiniaceae community composition in *M. digitata* juveniles
578 to be highly stable regardless of thermal exposure. This is in contrast to other studies in which
579 shuffling in juvenile corals has been repeatedly confirmed during initial symbiont acquisition
580 (Little et al. 2004; Yorifuji et al. 2017; Cumbo et al. 2013; Cumbo et al. 2013; Little et al. 2004;
581 Yorifuji et al. 2017), and through development (Quigley et al. 2017; 2020; Terrell et al. 2023),
582 only stabilizing later in life (Abrego et al. 2008). These changes through juvenile ontogeny are
583 generally referred to as winnowing (Abrego et al. 2008). Symbiont communities can change
584 during this winnowing period, and are characterised by increases in the abundance of opportunistic
585 symbionts influenced by environmental changes; however, dominant symbionts tend to
586 outcompete these opportunists through time (McIlroy et al. 2019). Although we saw community
587 differences in *M. digitata* larvae when exposed to heat stress, the contrasting stability of symbiont
588 communities in juveniles under the same conditions suggests that winnowing in this species may
589 occur earlier, possibly because symbiosis is initiated earlier, in oocytes. This further reinforces the
590 notion that the juvenile stage may be the most susceptible to stress. Further work is urgently needed
591 to better understand the dynamics of the symbiosis during this important ontogenetic transition.

592 **Variation in fitness among larval families and the role of symbiont community diversity**

593 To better understand parental contributions to fitness differences, we undertook controlled
594 genetic crosses. Previous work in this species showed a concordance between symbiont
595 communities in parents and their eggs (Quigley et al. 2019) and we were expecting similar patterns
596 in larvae – as we indeed observed here. Symbiont community is a heritable trait (Quigley et al.
597 2017; 2019), which implies that familial effects will be present. This has been demonstrated in a
598 number of species in the Indo-Pacific (*Acropora tenuis* and *Montipora digitata*, Quigley et al.
599 2017; *Seriatopora hystrix*, Quigley et al. 2018). Importantly, we also showed that differences in
600 symbiont communities among families are associated with differences in survival in larvae. In
601 particular, larvae from cross WT3xC1 exhibited lower average survival and had the most disparate
602 background symbiont community. This may have been due to the maternal influence of WT3,
603 which had a distinct endosymbiont community dominated by C15-C15dq-C15dr when compared
604 to the other three parental colonies. Therefore, poorer offspring survival could be due to increased
605 abundance of opportunistic *Cladocopium* spp. variants (Howe-Kerr et al. 2020). We lacked the
606 ability to measure the degree to which symbiont community differences among families can
607 change in response to heat stress due to low sample sizes. Further work is therefore needed to
608 determine if an increase in potentially opportunistic symbionts would increase or decrease the
609 capacity for coral early life stages of *M. digitata* to alter performance under heat stress.

610

611

612 **Conclusion**

613 Overall, we observed changes in symbiont communities in the early life stages of *M.*
614 *digitata* in response to heat stress. We could not determine if these changes were due to an active
615 or passive mechanism. However, our results suggest juvenile stages of *M. digitata* are more
616 susceptible to heat stress compared to the larval stage. In order to determine if shuffling is indeed
617 an active acclimatory mechanism, higher resolution time series sampling of early life stages should
618 be conducted. As rare taxa increased in abundance in larvae that were heat stressed, future studies
619 should also examine the degree to which background symbiont communities can be inherited,
620 which will require larger cross designs. As *M. digitata* is a vertically transmitting species, the
621 degree to which rare-heat tolerant species are inherited in offspring may be an indicator of their
622 future resistance to heat stress, which will play a critical role in their survival in a rapidly changing
623 climate.

624 **Acknowledgements**

625 We acknowledge and pay our respects to Manbarra Traditional Owners, whose
626 SeaCountry these corals were collected from. We would also like to acknowledge Dylan Skilton,
627 Magena Marzonie, Carys Morgans, Ole Brodnicke, Carly Randall, Carlos Alvarez Roa, and the
628 National Sea Simulator Staff at the Australian Institute of Marine Science for either fieldwork
629 support, coral spawning, or experimental support. We would also like to thank Dr's. Emily
630 Aguirre and Maria Ruggeri for support in library preparation training and Dr. Melissa Guzman
631 for support in statistical analysis. K.M.Q was supported by the Minderoo Foundation and an
632 ARC DECRA Fellowship (DE230100284).

633
634 **Data Availability**

635 All raw sequence reads can be found in SRA project PRJNA1112848 with a [token link](#).
636 Metadata and code can be found in our [Github](#) under a personal access token:
637 github_pat_11ATLNH2Y0VGiQcwKelQfB_DrAXUIEqF53O0eg1ROfE4X66gMjBhuNtFclL7
638 vB7YpV7ZQ4VD2cSZpdtmm

639
640
641

642

643

644

645

646

647 **References**

- 648 Abrego, D., K. E. Ulstrup, B. L. Willis, and M. J. H. van Oppen. 2008. Species-specific
649 interactions between algal endosymbionts and coral hosts define their bleaching response to
650 heat and light stress. *Proc. Biol. Sci.* 275:2273–2282.
- 651 Aranda, M., A. T. Banaszak, T. Bayer, J. R. Luyten, M. Medina, and C. R. Voolstra. 2011.
652 Differential sensitivity of coral larvae to natural levels of ultraviolet radiation during the
653 onset of larval competence. *Mol. Ecol.* 20:2955–2972.
- 654 Baird, A. H., J. R. Guest, and B. L. Willis. 2009. Systematic and Biogeographical Patterns in the
655 Reproductive Biology of Scleractinian Corals. *Annu. Rev. Ecol. Evol. Syst.* 40:551–571.
656 Annual Reviews.
- 657 Baker, A. C. 2001. Reef corals bleach to survive change. *Nature* 411:765–766. nature.com.
- 658 Baker, A. C. 2004. Symbiont diversity on coral reefs and its relationship to bleaching resistance
659 and resilience. *Coral health and disease*. Springer.
- 660 Baker, A. C., C. J. Starger, T. R. McClanahan, and P. W. Glynn. 2004. Corals’ adaptive response
661 to climate change. *Nature*. nature.com.
- 662 Berkelmans, R., and M. J. H. Van Oppen. 2006. The role of zooxanthellae in the thermal
663 tolerance of corals: a “nugget of hope” for coral reefs in an era of climate change.
664 *Proceedings of the. royalsocietypublishing.org*.
- 665 Björk, J. R., C. Díez-Vives, C. Astudillo-García, E. A. Archie, and J. M. Montoya. 2019.
666 Vertical transmission of sponge microbiota is inconsistent and unfaithful. *Nat Ecol Evol*
667 3:1172–1183.
- 668 Bushnell, B. 2020. BBDuk. [/bbtools/bb-tools-userguide/bbduk-guide/](http://bbtools/bb-tools-userguide/bbduk-guide/)(accessed on
- 669 Callahan, B. J., P. J. McMurdie, M. J. Rosen, A. W. Han, A. J. A. Johnson, and S. P. Holmes.

670 2016. DADA2: High-resolution sample inference from Illumina amplicon data. *Nat.*
671 *Methods* 13:581–583. [nature.com](https://doi.org/10.1038/nmeth.3326).

672 Cumbo, V. R., A. H. Baird, and M. J. H. van Oppen. 2013. The promiscuous larvae: flexibility in
673 the establishment of symbiosis in corals. *Coral Reefs* 32:111–120. Springer Science and
674 Business Media LLC.

675 Cunning, R., R. N. Silverstein, and A. C. Baker. 2018. Symbiont shuffling linked to differential
676 photochemical dynamics of Symbiodinium in three Caribbean reef corals. *Coral Reefs*
677 37:145–152. Springer.

678 Davies, S. W., M. H. Gamache, L. I. Howe-Kerr, N. G. Kriefall, A. C. Baker, A. T. Banaszak, L.
679 K. Bay, A. J. Bellantuono, D. Bhattacharya, C. X. Chan, D. C. Claar, M. A. Coffroth, R.
680 Cunning, S. K. Davy, J. Del Campo, E. M. Díaz-Almeyda, J. C. Frommlet, L. E. Fuess, R.
681 A. González-Pech, T. L. Goulet, K. D. Hoadley, E. J. Howells, B. C. C. Hume, D. W.
682 Kemp, C. D. Kenkel, S. A. Kitchen, T. C. LaJeunesse, S. Lin, S. E. McIlroy, R. McMinds,
683 M. R. Nitschke, C. A. Oakley, R. S. Peixoto, C. Prada, H. M. Putnam, K. Quigley, H. G.
684 Reich, J. D. Reimer, M. Rodriguez-Lanetty, S. M. Rosales, O. S. Saad, E. M. Sampayo, S.
685 R. Santos, E. Shoguchi, E. G. Smith, M. Stat, T. G. Stephens, M. E. Strader, D. J. Suggett,
686 T. D. Swain, C. Tran, N. Traylor-Knowles, C. R. Voolstra, M. E. Warner, V. M. Weis, R.
687 M. Wright, T. Xiang, H. Yamashita, M. Ziegler, A. M. S. Correa, and J. E. Parkinson. 2023.
688 Building consensus around the assessment and interpretation of Symbiodiniaceae diversity.
689 *PeerJ* 11:e15023.

690 Davy Simon K., Allemand Denis, and Weis Virginia M. 2012. Cell Biology of Cnidarian-
691 Dinoflagellate Symbiosis. *Microbiol. Mol. Biol. Rev.* 76:229–261. American Society for
692 Microbiology.

693 Davy, S. K., and J. R. Turner. 2003. Early development and acquisition of Zooxanthellae in the
694 temperate symbiotic sea anemone *Anthopleura ballii* (Cocks). *Biol. Bull.* 205:66–72.

695 Dixon, G. B., and C. D. Kenkel. 2019. Molecular convergence and positive selection associated
696 with the evolution of symbiont transmission mode in stony corals. *Proc. Biol. Sci.*
697 286:20190111.

698 Ebert, D. 2013. The Epidemiology and Evolution of Symbionts with Mixed-Mode Transmission.
699 *Annu. Rev. Ecol. Evol. Syst.* 44:623–643. Annual Reviews.

700 Edmunds, P., R. Gates, and D. Gleason. 2001. The biology of larvae from the reef coral *Porites*
701 *astreoides*, and their response to temperature disturbances. *Mar. Biol.* 139:981–989.
702 Springer.

703 Elder, H., W. C. Million, E. Bartels, C. J. Krediet, E. M. Muller, and C. D. Kenkel. 2023. Long-
704 term maintenance of a heterologous symbiont association in *Acropora palmata* on natural
705 reefs. *ISME J.* 17:486–489. [nature.com](https://doi.org/10.1038/s41564-023-01111-1).

706 Fabina, N. S., H. M. Putnam, E. C. Franklin, M. Stat, and R. D. Gates. 2012. Transmission mode
707 predicts specificity and interaction patterns in coral-Symbiodinium networks. *PLoS One*
708 7:e44970. [journals.plos.org](https://doi.org/10.1371/journal.plosone.0174970).

709 Fuller, Z. L., V. J. L. Mocellin, L. A. Morris, N. Cantin, J. Shepherd, L. Sarre, J. Peng, Y. Liao,
710 J. Pickrell, P. Andolfatto, M. Matz, L. K. Bay, and M. Przeworski. 2020. Population
711 genetics of the coral *Acropora millepora*: Toward genomic prediction of bleaching. *Science*
712 369:eaba4674.

713 Gleason, D. F., and D. K. Hofmann. 2011. Coral larvae: From gametes to recruits. *J. Exp. Mar.*
714 *Bio. Ecol.* 408:42–57. Elsevier.

715 Glynn, P. W. 1993. Coral reef bleaching: ecological perspectives. *Coral Reefs* 12:1–17. Springer.

716 Hirose, M., and M. Hidaka. 2006. Early development of zooxanthella-containing eggs of the
717 corals *Porites cylindrica* and *Montipora digitata*: The endodermal localization of
718 zooxanthellae. *Zoolog. Sci.* 23:873–881. BioOne.

719 Howe-Kerr, L. I., B. Bachelot, R. M. Wright, C. D. Kenkel, L. K. Bay, and A. M. S. Correa.
720 2020. Symbiont community diversity is more variable in corals that respond poorly to
721 stress. *Glob. Chang. Biol.* 26:2220–2234.

722 Hume, B. C. C., E. G. Smith, M. Ziegler, H. J. M. Warrington, J. A. Burt, T. C. LaJeunesse, J.
723 Wiedenmann, and C. R. Voolstra. 2019. SymPortal: A novel analytical framework and
724 platform for coral algal symbiont next-generation sequencing ITS2 profiling. *Mol. Ecol.*
725 *Resour.* 19:1063–1080. Wiley.

726 Kiers, E. T., R. A. Rousseau, S. A. West, and R. F. Denison. 2003. Host sanctions and the
727 legume–rhizobium mutualism. *Nature* 425:78–81. Nature Publishing Group.

728 Krueger, T., and R. D. Gates. 2012. Cultivating endosymbionts — Host environmental mimics
729 support the survival of *Symbiodinium* C15 ex hospite. *J. Exp. Mar. Bio. Ecol.* 413:169–176.
730 Elsevier BV.

731 LaJeunesse, T. C., J. E. Parkinson, P. W. Gabrielson, H. J. Jeong, J. D. Reimer, C. R. Voolstra,
732 and S. R. Santos. 2018. Systematic Revision of Symbiodiniaceae Highlights the Antiquity
733 and Diversity of Coral Endosymbionts. *Curr. Biol.* 28:2570–2580.e6.

734 Lesser, M. P. 2019. Phylogenetic signature of light and thermal stress for the endosymbiotic
735 dinoflagellates of corals (Family Symbiodiniaceae). *Limnol. Oceanogr.* 64:1852–1863.
736 Wiley.

737 Little, A. F., M. J. H. van Oppen, and B. L. Willis. 2004. Flexibility in algal endosymbioses
738 shapes growth in reef corals. *Science* 304:1492–1494. science.org.

739 Martin, M. 2011. Cutadapt removes adapter sequences from high-throughput sequencing reads.
740 EMBnet.journal 17:10–12. journal.embnet.org.

741 Matsuda, S. B., L. J. Chakravarti, R. Cunning, A. S. Huffmyer, C. E. Nelson, R. D. Gates, and
742 M. J. H. van Oppen. 2022. Temperature-mediated acquisition of rare heterologous
743 symbionts promotes survival of coral larvae under ocean warming. *Glob. Chang. Biol.*
744 28:2006–2025. Wiley.

745 McIlroy SE, Cunning R, Baker AC, Coffroth MA. Competition and succession among coral
746 endosymbionts. *Ecol Evol.* 2019;9: 12767–12778.

747 McMurdie, P. J., and S. Holmes. 2013. phyloseq: an R package for reproducible interactive
748 analysis and graphics of microbiome census data. *PLoS One* 8:e61217. journals.plos.org.

749 Mieog, J. C., M. J. H. van Oppen, N. E. Cantin, W. T. Stam, and J. L. Olsen. 2007. Real-time
750 PCR reveals a high incidence of Symbiodinium clade D at low levels in four scleractinian
751 corals across the Great Barrier Reef: implications for symbiont shuffling. *Coral Reefs*
752 26:449–457. Springer.

753 Oksanen, J., R. Kindt, P. Legendre, B. O’Hara, M. H. H. Stevens, M. J. Oksanen, and M.
754 Suggests. 2007. The vegan package. *Community ecology package* 10:719. researchgate.net.

755 Padilla-Gamiño, J. L., X. Pochon, C. Bird, G. T. Concepcion, and R. D. Gates. 2012. From
756 parent to gamete: vertical transmission of Symbiodinium (Dinophyceae) ITS2 sequence
757 assemblages in the reef building coral *Montipora capitata*. *PLoS One* 7:e38440.
758 journals.plos.org.

759 Pechenik, J. A. 1999. On the advantages and disadvantages of larval stages in benthic marine
760 invertebrate life cycles. *Mar. Ecol. Prog. Ser.* 177:269–297. Inter-Research Science Center.

761 Peet, R. K. 1974. The Measurement of Species Diversity. *Annu. Rev. Ecol. Evol. Syst.* 5:285–

762 307. Annual Reviews.

763 Putnam, H. M., M. Stat, X. Pochon, and R. D. Gates. 2012. Endosymbiotic flexibility associates
764 with environmental sensitivity in scleractinian corals. *Proc. Biol. Sci.* 279:4352–4361.

765 Quigley, K. M., C. Alvarez-Roa, J. B. Raina, and M. Pernice. 2023. Heat-evolved microalgal
766 symbionts increase thermal bleaching tolerance of coral juveniles without a trade-off
767 against growth. *Coral Reefs*. Springer.

768 Quigley, K. M., C. Alvarez Roa, and G. Torda. 2020. Co-dynamics of Symbiodiniaceae and
769 bacterial populations during the first year of symbiosis with *Acropora tenuis* juveniles.
770 Wiley Online Library.

771 Quigley, K. M., B. Ramsby, P. Laffy, J. Harris, V. J. L. Mocellin, and L. K. Bay. 2022.
772 Symbioses are restructured by repeated mass coral bleaching. *Sci Adv* 8:eabq8349.

773 Quigley, K. M., P. A. Warner, L. K. Bay, and B. L. Willis. 2018. Unexpected mixed-mode
774 transmission and moderate genetic regulation of Symbiodinium communities in a brooding
775 coral. *Heredity* 121:524–536. [nature.com](https://www.nature.com).

776 Quigley, K. M., B. L. Willis, and L. K. Bay. 2017. Heritability of the Symbiodinium community
777 in vertically- and horizontally-transmitting broadcast spawning corals. *Sci. Rep.* 7:8219.

778 Quigley, K. M., B. L. Willis, and C. D. Kenkel. 2019. Transgenerational inheritance of shuffled
779 symbiont communities in the coral *Montipora digitata*. *Sci. Rep.* 9:13328.

780 Ritson-Williams, R., S. Arnold, N. Fogarty, R. S. Steneck, M. Vermeij, and V. J. Paul. 2009.
781 New perspectives on ecological mechanisms affecting coral recruitment on reefs. *Smithson.*
782 *Contrib. Mar. Sci.* 437–457. Smithsonian Institution.

783 Rodriguez-Lanetty, M., S. Harii, and O. Hoegh-Guldberg. 2009. Early molecular responses of
784 coral larvae to hyperthermal stress. *Mol. Ecol.* 18:5101–5114. Wiley.

785 Sachs, J. L., U. G. Mueller, T. P. Wilcox, and J. J. Bull. 2004. The evolution of cooperation. *Q.*
786 *Rev. Biol.* 79:135–160. journals.uchicago.edu.

787 Sampayo, E. M., T. Ridgway, L. Franceschinis, G. Roff, O. Hoegh-Guldberg, and S. Dove.
788 2016. Coral symbioses under prolonged environmental change: living near tolerance range
789 limits. *Sci. Rep.* 6:36271. nature.com.

790 Sørensen, M. E. S., A. J. Wood, D. D. Cameron, and M. A. Brockhurst. 2021. Rapid
791 compensatory evolution can rescue low fitness symbioses following partner switching.
792 *Curr. Biol.* 31:3721–3728.e4.

793 Swain, T. D., J. Chandler, V. Backman, and L. Marcelino. 2017. Consensus thermotolerance
794 ranking for 110 Symbiodinium phylotypes: an exemplar utilization of a novel iterative
795 partial-rank aggregation tool with broad application potential. *Funct. Ecol.* 31:172–183.
796 Wiley.

797 Swain, T. D., S. Lax, J. Gilbert, V. Backman, and L. A. Marcelino. 2021. A Phylogeny-Informed
798 Analysis of the Global Coral-Symbiodiniaceae Interaction Network Reveals that Traits
799 Correlated with Thermal Bleaching Are Specific to Symbiont Transmission Mode.
800 *mSystems* 6. Am Soc Microbiol.

801 Terrell, A. P., E. Marangon, N. S. Webster, I. Cooke, and K. M. Quigley. 2023. The promotion
802 of stress tolerant Symbiodiniaceae dominance in juveniles of two coral species under
803 simulated future conditions of ocean warming and acidification. *Frontiers in Ecology and*
804 *Evolution* 11. frontiersin.org.

805 Toby Kiers, E., T. M. Palmer, A. R. Ives, J. F. Bruno, and J. L. Bronstein. 2010. Mutualisms in a
806 changing world: an evolutionary perspective. *Ecol. Lett.* 13:1459–1474.

807 Torda, G., J. M. Donelson, M. Aranda, D. J. Barshis, L. Bay, M. L. Berumen, D. G. Bourne, N.

808 Cantin, S. Foret, M. Matz, D. J. Miller, A. Moya, H. M. Putnam, T. Ravasi, M. J. H. van
809 Oppen, R. V. Thurber, J. Vidal-Dupiol, C. R. Voolstra, S.-A. Watson, E. Whitelaw, B. L.
810 Willis, and P. L. Munday. 2017. Rapid adaptive responses to climate change in corals. *Nat.*
811 *Clim. Chang.* 7:627–636. Nature Publishing Group.

812 van Woesik, R. 2001. Coral bleaching: transcending spatial and temporal scales. *Trends Ecol.*
813 *Evol.* 16:119–121. Elsevier.

814 van Woesik, R., T. Shlesinger, A. G. Grottoli, R. J. Toonen, R. Vega Thurber, M. E. Warner, A.
815 Marie Hulver, L. Chapron, R. H. McLachlan, R. Albright, E. Crandall, T. M. DeCarlo, M.
816 K. Donovan, J. Eirin-Lopez, H. B. Harrison, S. F. Heron, D. Huang, A. Humanes, T.
817 Krueger, J. S. Madin, D. Manzello, L. C. McManus, M. Matz, E. M. Muller, M. Rodriguez-
818 Lanetty, M. Vega-Rodriguez, C. R. Voolstra, and J. Zaneveld. 2022. Coral-bleaching
819 responses to climate change across biological scales. *Glob. Chang. Biol.* 28:4229–4250.
820 Wiley.

821 Voolstra, C. R., J. J. Valenzuela, S. Turkarslan, A. Cárdenas, B. C. C. Hume, G. Perna, C.
822 Buitrago-López, K. Rowe, M. V. Orellana, N. S. Baliga, S. Paranjape, G. Banc-Prandi, J.
823 Bellworthy, M. Fine, S. Frias-Torres, and D. J. Barshis. 2021. Contrasting heat stress
824 response patterns of coral holobionts across the Red Sea suggest distinct mechanisms of
825 thermal tolerance. *Mol. Ecol.* 30:4466–4480.

826 Wellington, G. M., and W. K. Fitt. 2003. Influence of UV radiation on the survival of larvae
827 from broadcast-spawning reef corals. *Mar. Biol.* 143:1185–1192. Springer.

828 Yorifuji, M., S. Harii, R. Nakamura, and M. Fudo. 2017. Shift of symbiont communities in
829 *Acropora tenuis* juveniles under heat stress. *PeerJ.* peerj.com.

830 Yorifuji, M., H. Yamashita, G. Suzuki, T. Kawasaki, T. Tsukamoto, W. Okada, K. Tamura, R.

831 Nakamura, M. Inoue, M. Yamazaki, and S. Harii. 2021. Unique environmental
832 Symbiodiniaceae diversity at an isolated island in the northwestern Pacific. *Mol.*
833 *Phylogenet. Evol.* 161:107158. Elsevier.

834 Zhang, Y., W. C. Million, M. Ruggeri, and C. D. Kenkel. 2019. Family matters: Variation in the
835 physiology of brooded *Porites astreoides* larvae is driven by parent colony effects. *Comp.*
836 *Biochem. Physiol. A Mol. Integr. Physiol.* 238:110562.

837